IMPACT OF LACTATE ON EXOSOMES AND ITS ROLE IN ACUTE PANCREATITIS-ASSOCIATED INFLAMMATION

UNIVERSITY MASTER'S DEGREE IN BIOCHEMISTRY, MOLECULAR BIOLOGY AND BIOMEDICINE

2024-2025

Institut d'Investigacions Biomèdiques de Barcelona (IIBB-CSIC)

– Department of Experimental Pathology

Noemi Canalda Batalla

Supervised by Dr. Daniel Closa Autet

I would like to express my sincere gratitude to Dr. Daniel Closa for giving me the opportunity to collaborate on his project and sharing his knowledge with me throughout this process. I am deeply thankful for his guidance, patience, and the valuable advice he has offered me.

To Olga and Júlia, for teaching me with such dedication and for always being willing to help and guide me whenever I need it.

To my friends, for standing by my side, encouraging me, and being there when I needed it most.

To my mother and my father, for their endless love and unconditional support. Thank you for believing in me even when I didn't believe in myself, and for being proud of the person I am.

To my sister, my lifelong companion, for being my refuge and for the privilege of growing up by your side.

To my aunt Maite, for being a role model of strength, courage and boundless joy.

And to my grandparents, José and Luisa, my guardian angels. Even though they are no longer with me, I know they accompany me in every decision and are present in every step of my journey.

Abstract

Background: Acute pancreatitis (AP) is an inflammatory condition often associated with systemic complications, and macrophages are key regulators of the inflammatory response. Exosomes, a subtype of small extracellular vesicles (sEVs), are important mediators of intercellular crosstalk and can influence immune cell behavior. Lactated Ringer's solution (LR), commonly used in AP treatment, contains lactate, which has demonstrated anti-inflammatory effects. This study explores whether exosome exposure to lactate modifies their effect on macrophage inflammatory response.

Methods: Exosomes were isolated from human pancreatic BxPC3 cells and incubated with either different concentrations of lactate or with a fixed concentration equivalent to that present in LR, for different durations. Exosomes were characterized by nanoparticle tracking analysis and Western blot. THP-1-derived macrophages were treated with these exosomes. Macrophage pro- and anti-inflammatory gene expression was analyzed by RT-qPCR. Exosome uptake was assessed by fluorescence microscopy, and STAT3 localization was evaluated by immunofluorescence.

Results: Optimizing the exosome isolation protocol improved sEV yield and purity. Macrophages treated with lactate-exposed exosomes exhibited reduced expression of M1-associated markers (TNF-α, IL-1β) and increased expression of M2 markers (IL-10, MRC-1, ARG-1), suggesting a shift towards an anti-inflammatory phenotype. These effects were observed across all lactate concentration and exposure times, with just 10 minutes of incubation being sufficient to induce changes. STAT3 is not involved in the observed polarization. Exosome uptake was comparable between lactate-treated exosomes and control groups.

Conclusions: Lactate modifies exosomes properties, promoting macrophage polarization shift towards the M2 phenotype. This effect is independent of STAT3 activation or exosome internalization. These findings support an anti-inflammatory role of lactate mediated by exosomes and highlight a potential mechanism by which LR mitigates inflammation in AP.

Keywords: Inflammation, acute pancreatitis, small extracellular vesicles, exosomes, macrophage polarization, lactate.

INDEX

Abbreviations

AP: Acute Pancreatitis

ARG-1: Arginase-1

BSA: Bovine Serum Albumin

DMEM: Dulbecco's Modified Eagle Medium

DNA: Deoxyribonucleic Acid

ESCRT: Endosomal Sorting Complexes Required for Transport

EVs: Extracellular Vesicles

FBS: Fetal Bovine Serum

GAPDH: Glyceraldehyde-3-Phosphate Dehydrogenase

IFN-γ: Interferon-Gamma

IL-1β: Interleukin-1β

IL-4: Interleukin-4

IL-10: Interleukin-10

IL-13: Interleukin-13

iNOS: Inducible Nitric Oxide Synthase

LPS: Lipopolysaccharide

LR: Lactated Ringer’s Solution

MRC-1: Mannose Receptor C-type 1

NS: Normal Saline

ON: Over Night

PBS: Phosphate Buffered Saline

PC: Protein Corona

PMA: Phorbol 12-Myristate 13-Acetate

RNA: Ribonucleic Acid

RT-qPCR: Quantitative Reverse Transcription Polymerase Chain Reaction

sEVs: Small Extracellular Vesicles

SIRS: Systemic Inflammatory Response Syndrome

TBST: Tris-Buffered Saline with Tween 20

TNF-α: Tumor Necrosis Factor-α

1. Introduction

1.1. Inflammation

In response to injurious stimuli potentially causing tissue damage or disease, the immune system activates a defensive mechanism known as inflammatory response. This process aims to neutralize the source of harm and promote the restoration of tissue homeostasis by triggering intracellular signaling pathways that regulate the transcription of inflammatory genes. These genes induce the release of inflammatory mediators, which, in turn, recruit and activate immune cells at the damaged site[1]. In this entire process, macrophages play a determining role since they are responsible for orchestrating the response of the rest of the cell populations involved in both inflammation and the resolution of the process[2].

Macrophages are immune cells derived from monocytes and are capable of transitioning between different phenotypes in response to cues from the microenvironment. This process, known as macrophage polarization, gives rise to two principal macrophage subpopulations: M1, also known as pro-inflammatory, and M2, or anti-inflammatory. These phenotypes differ in surface marker expression, the specific factors they release, and their distinct biological functions[3]. Also, the plasticity of macrophages allows these differentiated cells to re-polarize and switch from one phenotype to the other depending on the environmental signals[4].

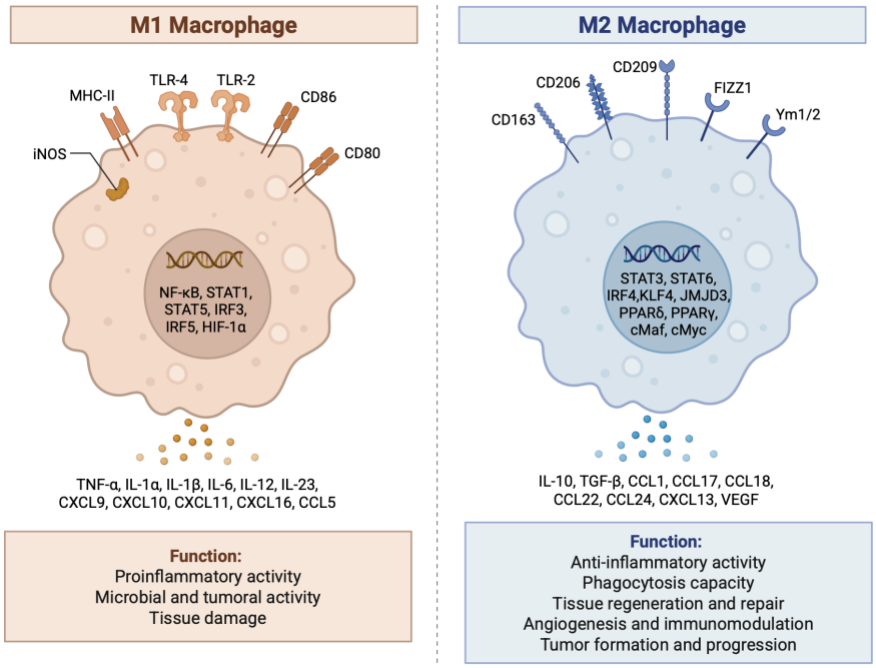

Figure 1: Schematic representation of M1 and M2 macrophages phenotypes. Adapted from: https://www.biorender.com/template/macrophage-polarization-m1-and-m2-subtypes, by BioRender.com (accessed on 15 June 2025).

Microbial products, such as lipopolysaccharide (LPS), and pro-inflammatory cytokines like interferon-gamma (IFN-γ) or tumor necrosis factor-α (TNF-α) induce macrophages to polarize towards the M1 phenotype, which, in turn, secrete pro-inflammatory cytokines including

interleukin-1β (IL-1β) and TNF-α, and induce enzymes like inducible nitric oxide synthase (iNOS). Regarding M2 phenotype, polarization is mainly induced by interleukin-4 (IL-4) and interleukin-13 (IL-13), stimulating the production of high levels of interleukin-10 (IL-10), mannose receptor c-type 1 (MRC-1) and enzimes like arginase-1 (ARG-1)[3].

During the early stages of inflammation, macrophages typically acquire an M1 phenotype to eliminate pathogens and initiate immune responses. As inflammation progresses towards resolution, macrophages transition to the M2 phenotype, which helps suppress inflammation and promotes tissue repair and regeneration[3].

1.2. Exosomes

Extracellular vesicles (EVs) are nanosized, membrane-enclosed structures surrounded by a lipid bilayer. They are released by all cell types and have been identified in all tissues and body fluids. Based on their size, EVs are classified as large EVs (>200 nm) or small EVs (<200 nm)[5].

Exosomes are a subtype of small extracellular vesicles (sEVs) released by almost all cell types, typically ranging in size from 30 to 150 nm in diameter[6]. These nanovesicles originate from invaginations of the late endosomal membrane, forming smaller internal vesicles that enclose cargo molecules, such as lipids, proteins and nucleic acids. These internal vesicles, known as intraluminal vesicles, become exosomes when the late endosome fuses with the cell's plasma membrane, leading to their release into the extracellular space.

Exosomes are important mediators of intercellular and interorgan communication, although they were initially considered a cellular mechanism to eliminate waste products. Once secreted, these sEVs travel through the circulatory system, enabling them to reach both nearby and distant target cells[7]. Exosomes form a heterogeneous population due to variations in size, molecular content, and cellular origin, which confer certain tropism to specific organs, preferential uptake by particular cell types, and diverse biological effects on target cells[8]. Upon reaching the recipient cell, these nanoparticles can influence intracellular signaling either by binding to surface receptors and triggering signaling cascades, by being internalized through different endocytic pathways (clathrin-mediated, caveolin-dependent, lipid raft-mediated, phagocytosis or macropinocytosis), or by directly fusing with the plasma membrane and release their cargo into the target cell's cytosol[9,10]. However, it remains unclear to what extent exosome targeting is random or cell-specific[9].

The membrane composition of exosomes varies depending on their cell of origin, which can change according to the cell's physiological condition[7]. Despite their heterogeneity, exosomes derived from different cell types share common proteins involved in their biogenesis, which are commonly used for their characterization[11]. Classical exosomal markers include tetraspiranes such as CD9 and CD63, and other proteins like TSG101 and Alix[7,10,12].

Exosomes are secreted under both physiological and pathological conditions and have emerged as relevant mediators implicated in different pathologies, including neurodegenerative and cardiovascular diseases[13]. However, their role has been extensively investigated in cancer[14] and inflammatory-related diseases[15]. Recent findings suggest that once exosomes are released into

biological fluids, they are exposed to a wide range of biomolecules, and the presence of specific molecules on the exosome surface can influence the binding of molecules to their surface. Interactions between the exosome surface and soluble proteins leads to the formation of a protein-rich outer layer known as protein corona (PC)[16]. The PC composition is strongly influenced by the surrounding microenvironment, and its formation can alter the biological properties and functions of sEVs[17,18]. The inflammatory microenvironment induces modifications in the exosomal PC as they circulate through the bloodstream[18], affecting exosome tropism and cellular uptake[19].

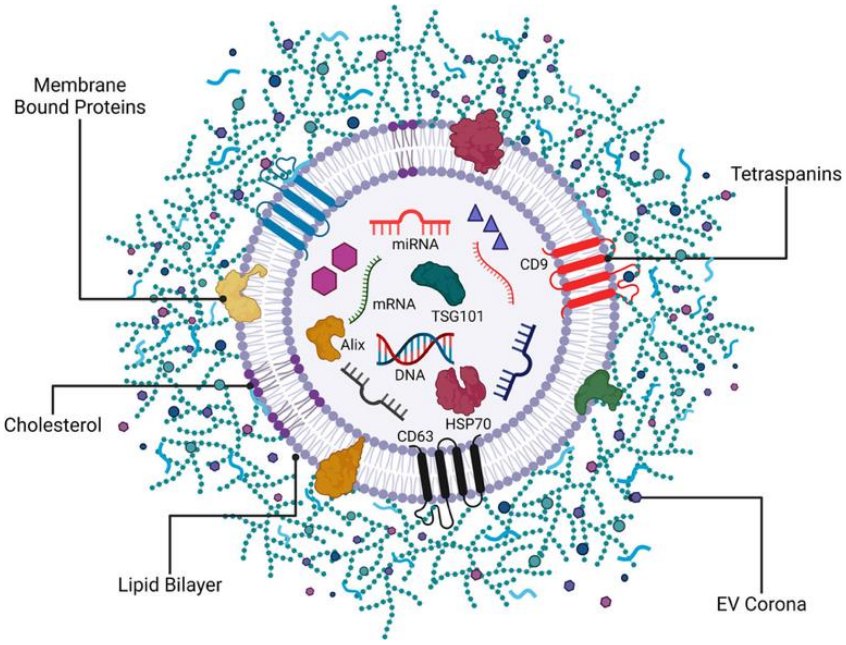

Figure 2: Illustrative representation of the classical morphology of a sEV, including the presence of an external protein corona[20].

1.3. Acute pancreatitis

Acute pancreatitis (AP) is an inflammatory disease of the pancreas resulting from multiple potential causes, though it is frequently associated with gallstones and alcohol abuse[21]. In the early stages of this inflammatory condition, the local cascade of pro-inflammatory cytokines within the pancreas may progress to a systemic response[22], initially manifesting as systemic inflammatory response syndrome (SIRS)[23]. Persistent SIRS increases the risk of organ failure[23], which is a key determinant of disease severity[24]. According to the revised Atlanta classification of AP, the disease is classified into three severity grades: mild, moderately severe, and severe. In its most severe form, it can be life-threatening due to a persistent organ failure lasting more than 48 hours, which may result in death[25].

Lung injury is a common complication of AP resulted by SIRS, and macrophages play a central role in lung dysfunction secondary to AP. A previous study of our group unveiled that exosomes released during AP reach alveolar cavity, promoting the activation of alveolar macrophages toward the pro-inflammatory phenotype[26]. Macrophages are one of the principal immune cells that take part in modulating the inflammation from its onset to its resolution. Their capacity to

dynamically adopt either a pro-inflammatory or anti-inflammatory phenotype highlights their involvement in progression of AP, making them potential targets for therapeutic approaches[2,27].

Fluid resuscitation is crucial for the management of AP. The most widely used intravenous solutions are lactated Ringer's solution (LR) and normal saline (NS), although there is an ongoing debate over which is the optimal fluid choice for administration. One of the main differences between the two solutions is that LR contains lactate, while NS does not. Prior studies concluded that LR administration was associated with decreased inflammation, an effect not observed when using LR without lactate[28,29]. Additionally, some short-chain fatty acids, including lactate, are known to reduce the inflammatory response[29].

Considering the anti-inflammatory effects of lactate and the fact that the PC of exosomes can be modified based on the surrounding microenvironment, it is reasonable to suggest that lactate may induce functional changes in exosomes. These, in turn, could modulate the activation and polarization of macrophages, ultimately contributing to the reduction of both lung and pancreatic inflammation.

2. Initial hypothesis and objectives

The central hypothesis of this study is that ***alterations induced by lactate in exosomes influence the activation of macrophages***. Therefore, the principal purpose of this project is to assess how exposure of exosomes to lactate affects the expression of specific pro-inflammatory cytokines in macrophages.

The specific aims of this study are:

- To improve the methodology for exosomes purification.
- To evaluate the effect of lactate treatment on the exosome-induced response in macrophages.
- To determine if lactate concentration modulates the inflammatory response in macrophages.
- To assess whether the duration of exosome exposure to lactate affects the expression of inflammatory genes in macrophages.
- To analyze the effect of lactate-treated exosomes on their uptake by macrophages.

3. Methodology

3.1. Cellular lines

Human pancreatic BxPC3 cells (ATCC, Manassas, VA, USA) were cultured in DMEM medium (Sigma-Aldrich, St. Louis, MO, USA) supplemented with 10% fetal bovine serum (FBS; Thermo Fisher Scientific, Waltham, MA, USA), 100 U/ml penicillin, and 100 µg/ml streptomycin. When cells reached 80% of confluence, the medium was removed and replaced with DMEM without FBS to avoid the interference of the exosomes present in FBS. After 72 hours, this exosome-free medium was collected and centrifuged at 1,000 x g for 3 minutes, and the supernatant (approximately 25ml) was collected in another tube and stored at -20°C. Additionally, at 80% confluence, cells were detached from the flask surface using trypsin and then subcultured.

Human monocytic THP-1 cells (ATCC, Manassas, VA, USA) were cultured in suspension in RPMI 1640 medium (Sigma-Aldrich, St. Louis, MO, USA) supplemented with 10% FBS, 100 U/ml penicillin, and 100 µg/ml streptomycin and 2.5 µg/ml amphotericin. Cells were incubated with 100 nM phorbol 12-myristate 13-acetate (PMA; Merck, Darmstadt, Germany) for 24 hours to induce differentiation into macrophages. Following this initial incubation, the PMA-containing medium was discarded, and after washing with Phosphate-Buffered Saline (PBS), the medium was replaced with fresh RPMI 1640 medium supplemented with FBS for an additional 24 hours before initiating the experiments.

Both cell lines were maintained in a humidified incubator at 37°C, 5% CO2 and 95% O2.

3.2. Exosome isolation and treatment

To isolate exosomes derived from BxPC3, the cell culture medium (approximately 25ml) was collected and centrifuged at 10,000 x g during 30 min at 4°C. Then, the supernatant was filtered through a 0.22 µm sterile filters (Millipore, Burlington, MA, USA) to eliminate cell debris. Samples were then ultracentrifuged at 100,000 x g for 2 or 16 hours at 4°C in an ultracentrifuge (Sorvall™ WX, Thermo Fisher Scientific, Waltham, MA, USA). The supernatant was aspirated, leaving the last 200-400 µl, which were resuspended in 25 ml of PBS. A second ultracentrifugation was performed at 100,000 x g for 2 or 5 hours at 4°C. The supernatant of all tubes was aspirated again, and the final 100-200 µl containing the exosomes were pooled into a 1.5 ml Eppendorf tube. The quality of the purified exosomes was evaluated by analyzing particle size and concentration by nanoparticle tracking analysis, and the total amount of exosomes obtained was quantified by measuring protein content by BCA assay.

To carry out the cellular experiments, the required amount of exosomes was incubated at 37°C in a heating chamber with the same volume of PBS (sEV-PBS) or three different concentrations of sodium lactate (sEV-L; Merck, Darmstadt, Germany): 1/3x, 1x and 3x. All concentrations were calculated based on the sodium lactate concentration present in RL, which is 312 mg/100 ml. The incubation time was 10 minutes, 1 hour, 5 hours or 24 hours. After the incubation period, the samples were filtered using 300 KDa Nanosep centrifugal devices (Sartorius, Göttingen, DE) by centrifugation at 12,200 x g for 3 minutes at room temperature. Exosomes were then washed with PBS, and the final 25 µl of pelleted exosomes were resuspended in 100 µl of PBS and transferred

into different 1.5 ml Eppendorf tubes, properly labelled according to the incubation condition samples were stored at -20°C.

3.3. Protein quantification by BCA

Exosomes were quantified using the Pierce BCA Protein Assay Kit (Thermo Fisher Scientific, Waltham, MA, USA), and a standard curve was generated using bovine serum albumin (BSA). The exosome sample was diluted 1:5 in PBS. A volume of 20 µl from each sample and standard was loaded in duplicate into a 96-well plate (Thermo Fisher Scientific, Waltham, MA, USA) and mixed with 200 µl of BCA reagent. The mixtures were incubated at 37°C for 1 hour in a heating chamber. Absorbance was then measured at 562 nm using a Multiskan™ SkyHigh microplate spectrophotometer (Thermo Fisher Scientific, Waltham, MA, USA) to quantify protein content.

3.4. Nanoparticle tracking analysis

Exosome concentration and size distribution were analyzed in the SOFT/U6 Nanbiosis service, using a NanoSight NS300 instrument (NanoSight, Malvern, UK). Identical parameters were applied to all samples and three 1-min-long videos were recorded for each. The background signal was assessed using filtered PBS, which showed no detectable particle presence.

3.5. Western blot analysis

10 µg of exosome sample were mixed with the loading buffer and the reducer agent. This mixture was denaturized at 95°C for 10 minutes. 2.5 µl of molecular weight marker (Chameleon Duo Pre-stained Protein Ladder, LI-COR Biosciences, Lincoln, NE, USA) and 25 µl of the exosome sample were loaded into a 4-12% protein gel (Invitrogen™, NuPAGE™ 4 to 12%, Bis-Tris, 1.0–1.5 mm, Thermo Fisher Scientific, Waltham, MA, USA).

The running buffer (NuPAGE SDS Running Buffer 20X, Thermo Fisher Scientific, Waltham, MA, USA) was added into the gel tank, and electrophoresis was carried out at 150 V for 1 hour. Then, proteins were transferred to a membrane using the iBlot Dry Blotting Gel Transfer System, as a transfer system program (Invitrogen, Waltham, MA, USA). The membranes were stained in red with Ponceau S Staining Solution red (Thermo Fisher Scientific, Waltham, MA, USA) to confirm successfully protein transfer and then washed. Blocking of the membranes was performed with 5% dry milk in TBST for 1 hour at room temperature. After that, membranes were sectioned and incubated overnight (ON) at 4°C with primary antibodies diluted in blocking buffer. The primary antibodies used were against TSG101 (ProteinTech, Rosemont, IL, USA), Alix (ProteinTech, Rosemont, IL, USA), CD9 (ProteinTech, Rosemont, IL, USA) and Calnexin (ProteinTech, Rosemont, IL, USA). All primary antibodies were diluted 1:500, except for the anti-calnexin antibody, which was diluted 1:1000.

The next day, the membranes were washed four times and incubated with IRDyLight 800-conjugated secondary antibody (LI-COR Biosciences, Lincoln, NE, USA), diluted 1:10,000, for 45 minutes at room temperature. Immunoreactive bands were visualized using Odyssey Infrared Imaging System (LI-COR Biosciences, Lincoln, NE, USA).

3.6. Cells treatments

Macrophage-differentiated THP-1 cells were incubated with 10 µg/ml of exosomes previously incubated with lactate (sEV-$L_{1/3x}$, sEV-L_{1x} or sEV-L_{3x}) or with PBS as a negative control (sEV-PBS) for 5 hours. As a positive control, cells were treated with 5 µg/ml of LPS for 3 hours, and as a basal control, cells not treated with exosomes. Each experimental condition was done for triplicate, and experiments were repeated three times over three different weeks. The expression levels of inflammatory cytokines were measured by RT-qPCR.

3.7. RT-qPCR

TRIzol reagent (Invitrogen; Carlsbad, CA, USA) was used for the cellular RNA extraction. Total RNA was quantified by measuring the absorbance at 260 and 280 nm using a NanoDrop ND-1000 spectrophotometer (NanoDrop Technologies, Wilmington, DE, USA), and the cDNA was synthesized from 1 µg RNA sample using the NZY First-Strand cDNA synthesis kit (NZYtech). The cDNA amplification by quantitative polymerase chain reaction (qPCR) was performed in a DNA Engine, Peltier Thermal Cycler (Bio-Rad, Hercules, CA, USA), using iTaqTM Universal SYBR® Green Supermix (Bio-rad, Hercules, CA, USA) and the corresponding human primers (supplementary material, Table S1). The amplification protocol is detailed in the supplementary material (supplementary material, Table S2). The specificity of the products was verified through melting curve analysis. The threshold cycle values were normalized to the expression of GAPDH as reference gene GAPDH using the ΔC(t) formula.

3.8. Exosomes and cells staining and cell uptake analysis

THP-1 cells were cultured in a lab-tek chamber (Sigma-Aldrich, St. Louis, MO, USA) and incubated ON in a humidified incubator at 37°C, 5% CO2 and 95% O2. The next day, medium of all wells was removed and replaced with fresh RPMI medium supplemented with FBS. After 24 hours, experiments were carried out.

To monitor exosomes uptake, both exosomes and cells were stained. 10 µg/ml of sEV-PBS and sEV-L_{1x} were stained with the PKH26 red fluorescent cell linker dye (Sigma-Aldrich, St. Louis, MO, USA) for 4 minutes. To remove the unbound dye, exosomes were filtered using 300 KDa Nanosep centrifugal devices (Sartorius, Göttingen, DE) by centrifugation at 12,200 x g for 3 minutes at room temperature. Exosomes were then washed with PBS, and the final 25 µl of stained exosomes were resuspended in 100 µl of PBS.

Cells were labelled with PKH67 green fluorescent cell linker dye (Sigma-Aldrich, St. Louis, MO, USA) for 4 minutes. The reaction was stopped with 3% BSA for 1 minute, and then, 200 µl of fresh RPMI medium supplemented with FBS were added to remove the excess dye. After this, the medium containing PKH67 and BSA was removed and replaced with another 200 µl of fresh RPMI medium supplemented with FBS. Then, cell cultures were treated during 1 hour with 10 µg/ml of the PBS and incubated with lactate treated exosomes. After this incubation, the medium was eliminated, and cell nucleus were stained in blue with Hoechst33342 (Thermo Fisher, Waltham, MA, USA). Finally, cells were washed three times with PBS and fixed using Mowiol (Sigma-Aldrich, St. Louis, MO, USA). The preparation was stored at -20°C.

3.9. Fluorescence microscopy and analysis

An inverted Nikon Eclipse Ti2-E microscope (Nikon Instruments, Melville, NY, USA), equipped with an Andor Dragonfly spinning disk unit and a high magnification NIKON 60x NA 1.4 objective, was used to observe the stained cells and exosomes, which were excited using fluorescent laser diodes at 405 nm and 488 nm. Images were captured with a high-resolution camera (Zyla 4.2, 2.0 Andor; Oxford Instruments Company, Belfast, UK). ImageJ open-source software version 1.54p was used to process and analyze images.

3.10. Immunofluorescence analysis

To evaluate STAT3 translocation, THP-1 cells were cultured in a lab-tek chamber (Sigma-Aldrich, St. Louis, MO, USA) and incubated ON in a humidified incubator at 37°C, 5% CO2 and 95% O2. The next day, medium of all wells was removed and replaced with fresh RPMI medium supplemented with FBS. After 24 hours, cells were treated either with 10 µg/ml of sEV-PBS or sEV-L_{1x} for one and a half hours.

Cells were fixed with 3.5% formaldehyde for 5 min at room temperature and afterwards incubated with anti-STAT3 primary antibody. Alexa fluor 488-conjugated anti-mouse was used as secondary antibody. Localization of STAT3 was determined via fluorescence microscopy.

3.11. Statistical analysis

GraphPad Prism software v. 4.02 was used to perform all statistical analyses, and data are presented as mean ± SEM. Data were analyzed using a two-tailed Student's t-test for comparing the different condition groups with controls and with sEV-PBS. Statistically significant differences were considered when $p < 0.05$.

4. Results

4.1. sEVs characterization

The NanoSight analysis provided the number and average size of the particles present in the sEV sample. Most sEVs were distributed around 100-200 nm, consistent with the expected size range of exosomes, and showed a predominant diameter of 135 nm (Figure 3).

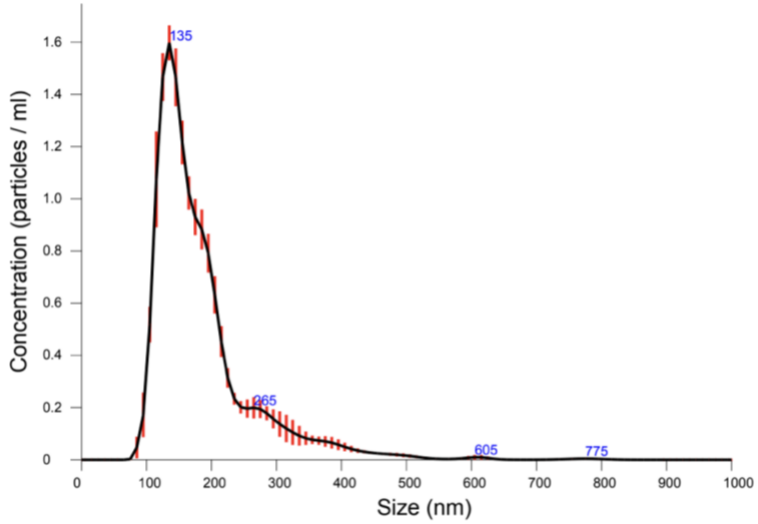

Figure 3: NanoSight profile of exosomes isolated from BxPC3 cells. The graph illustrates the particle size distribution on the X-axis, and the particle concentration on the Y-axis.

Western blot analysis of specific exosomal markers was performed to assess the quality of the isolated sEVs. Bands corresponding to the exosomal markers TSG101 (50 kDa), Alix (96 KDa) and CD9 (24 KDa) were detected. Finally, the absence of calnexin signal, an endoplasmic reticulum-associated protein, confirmed that the samples were not contaminated with vesicles from other subcellular compartments. Together, these results validate the purity of the isolated exosomes (Figure 4).

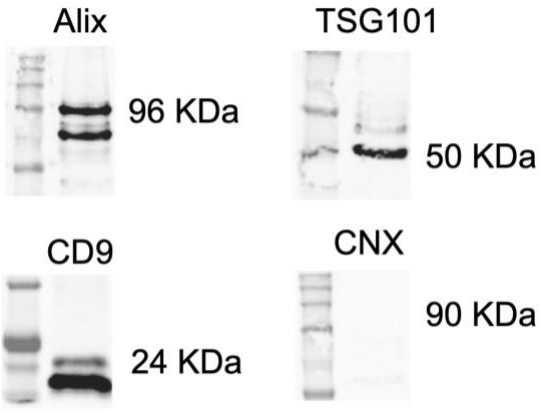

Figure 4: Western blot analysis of exosomes isolated from BxPC3 cells. Each lane was loaded with 10µg of protein, and 2.5µl of Chameleon Duo were used as the protein marker.

4.2. Improvement of exosomes isolating process

Given that exosomes are derived from cell culture medium, which contains a variety of soluble proteins, there is a risk that these proteins may co-isolate with the sEVs during the extraction process, compromising the purity of the final preparation[30].

For this reason, we assessed the efficiency of the existing isolation procedure in removing soluble proteins. To do so, different aliquots were collected at different stages throughout the isolating protocol in order to subsequently quantified particle number at each step, as schematically illustrated in Figure 5.

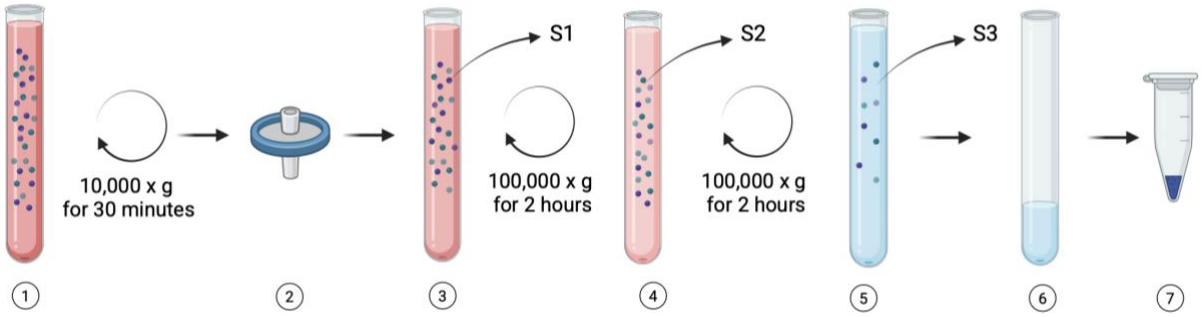

Figure 5: Schematic representation of the aliquots collected during sEV isolation process. BxPC3 cell culture is centrifuged at 10,000 x g for 30 minutes (1), followed by filtration through 0.22 µm filters (2, 3). The filtrate undergoes two rounds of ultracentrifugation at 100,000 x g for 2 hours (4, 5). The supernatant is discarded (6) and the final pellet is recovered (7). S1, S2 and S3 represent the aliquots collected. Created with BioRender.com.

The collected aliquots were taken from the supernatant, allowing us to determine the percentage of proteins removed during each phase. BCA assay (Figure 6) revealed that 81% of soluble proteins remained in the sample after the first 2-hour ultracentrifugation (S2), while only 1.71% of proteins persisted after the second 2-hour ultracentrifugation step (S3).

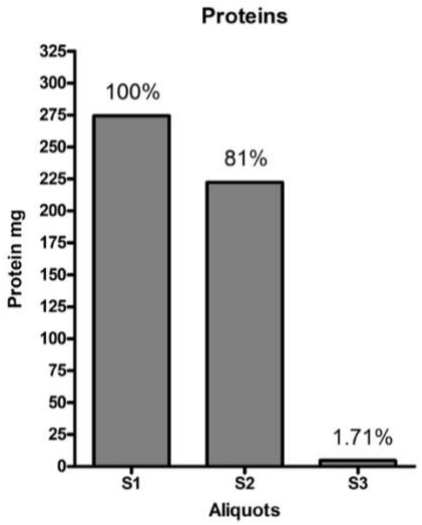

Figure 6: Quantification of soluble proteins by BCA assay. Aliquots were collected after the supernatant filtration step (S1), after the first 2-hour ultracentrifugation (S2), and after the second and final 2-hour ultracentrifugation (S3). The percentage of remaining particles present in each sample is indicated above the graph bars, all expressed relative to the initial particle amount (S1 sample set as 100%).

We also quantified the particle number present in the final sEV preparation obtained after the entire isolation procedure. Using these data, we calculated the ratio of sEV particle number to soluble protein content and compared its variation from the beginning to the end of the process (Table 1). After the first ultracentrifugation step, the ratio was very low (0.01). Conversely, after the final ultracentrifugation, the ratio notably increased to 103.62, reflecting that for every soluble protein present in the final sample, there were approximately 103 sEV particles.

	sEV/Soluble proteins
Initial (sEV/S1)	0.01
Final (sEV/S3)	103.62

Table 1: Ratio of exosome to soluble proteins at the initial (S1) and final steps (S3) of the isolation process.

After evaluating the efficiency of the method in removing soluble proteins, we then focused on evaluating its efficiency in terms of sEVs collection to determine if the protocol could be improved without compromising sample purity. For this purpose, we performed and compared two independent ultracentrifugation protocols differing in duration. During each procedure, aliquots were collected at different steps of the protocol, and the number and size of particles were determined through NanoSight analysis.

The ultracentrifugation times for each experimental condition were as follows: in the first assay, both the initial and final ultracentrifugation steps consisted of 2 hours (2h + 2h), while in the second condition, the first ultracentrifugation lasted 16 hours (ON), followed by a final spin of 5 hours (16h + 5h).

Despite starting with a higher particle number in the initial sample, the final sample obtained with the 2h + 2h condition resulted in a lower final number of particles compared to the 16h + 5h protocol (Figure 7). This increase is clearly confirmed by the comparative overlay in Figure 8, where the orange curve corresponding to the 16h + 5h exceeds the blue curve (2h + 2h).

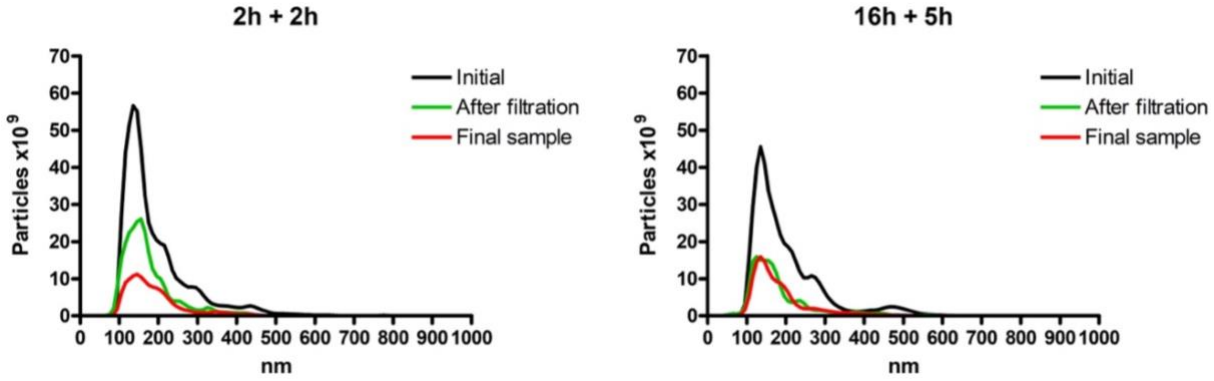

Figure 7: Nanosight analysis of two ultracentrifugation protocols used for sEV isolation. The black, green and red lines represent the initial sample, the sample after filtration and the final preparation, respectively.

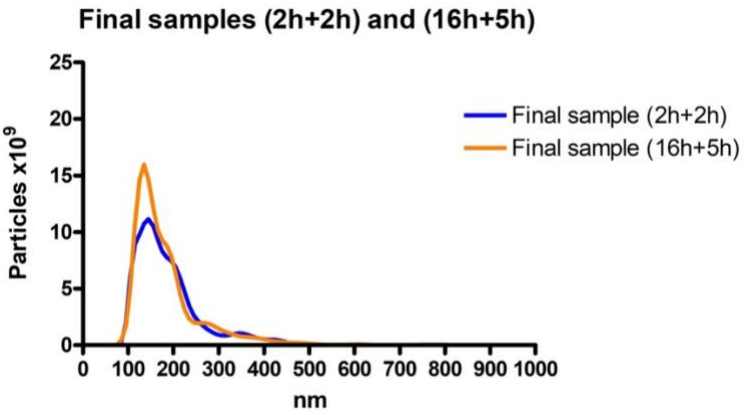

Figure 8: Nanosight analysis of the final samples obtained from the two ultracentrifugation protocols. The blue line represents the final sample of the 2h + 2h protocol, while the orange line corresponds to the final sample of the 16h + 5h protocol.

Although both assays resulted in particles with a peak ranging 100-200 nm, the particle size distribution obtained with the 16h + 5h condition was narrower, indicating a more homogeneous population of sEVs.

4.3. Effect of lactate on sEVs

4.3.1 Changes in macrophage gene expression induced by lactate-treated exosomes

To evaluate how lactate might influence macrophage gene expression through exosomes, we conducted experiments in which sEVs were treated with the lactate concentration present in RL.

These lactate-treated exosomes (sEV-L_{1x}) were incubated with THP-1-derived macrophages for 5 hours. After this period, the expression levels of typical M1 macrophage markers was assessed, including *IL-1β* and *TNF-α*. As experimental controls, we used untreated THP-1-derived macrophages (basal control), and cells treated with exosomes previously incubated with PBS (sEV-PBS, negative control).

The gene expression analysis showed a reduction in the expression of classical M1 phenotype markers in cells treated with sEV-L_{1x} compared to both control groups, whereas cells exposed to sEV-PBS revealed a slight increase in the expression of these markers relative to the untreated control, as represented in Figure 9.

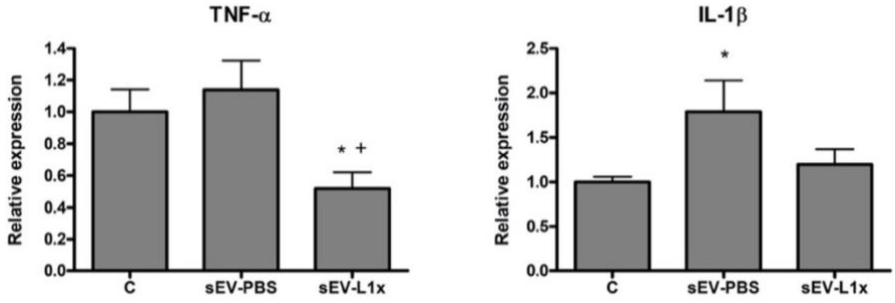

*Figure 9: Relative expression levels of TNF-α and IL-1β in THP-1-derived macrophages treated with sEVs previously incubated with PBS (sEV-PBS) or lactate (sEV-L1x). Control cells (C) were not exposed to sEVs. Cells were incubated with the respective treatment for 5 hours. *p<0.05 vs Control; +p<0.05 vs sEV-PBS.*

The data suggests a tendency towards increased expression of *TNF-α* and *IL-1β* in macrophages treated with sEV-PBS compared to untreated cells. This effect was reversed when cells were treated with sEV-L_{1x}.

4.3.2 Influence of lactate concentration on exosomes

Following the previous results, we hypothesized that increasing lactate concentration for the exosomes treatment could lead to more pronounced changes of M1 expression genes. We also evaluated the expression levels of the classical M2 markers and calculated the *IL-10/IL-1β*, *ARG-1/iNOS* and *MRC-1/TNF-α* ratios to evaluate a potential switch to an M2 phenotype.

To test it, exosomes were incubated with three lactate concentrations, all calculated based on the lactate concentration found in LR, which is 312 mg/100 ml: three times higher (L_{3x}), three times lower ($L_{1/3x}$) and the same concentration present in LR (L_{1x}).

As observed in Figure 10, the expression of classical M1 markers was decreased in macrophages treated with sEV-L compared to both the untreated control cells and those treated with sEV-PBS. In contrast, M2-associated markers showed an increased expression in the sEV-L-treated cells relative to the sEV-PBS and untreated conditions. This pattern was further supported by the elevated M2/M1 ratio, reflecting the upregulation of M2 markers under lactate conditions.

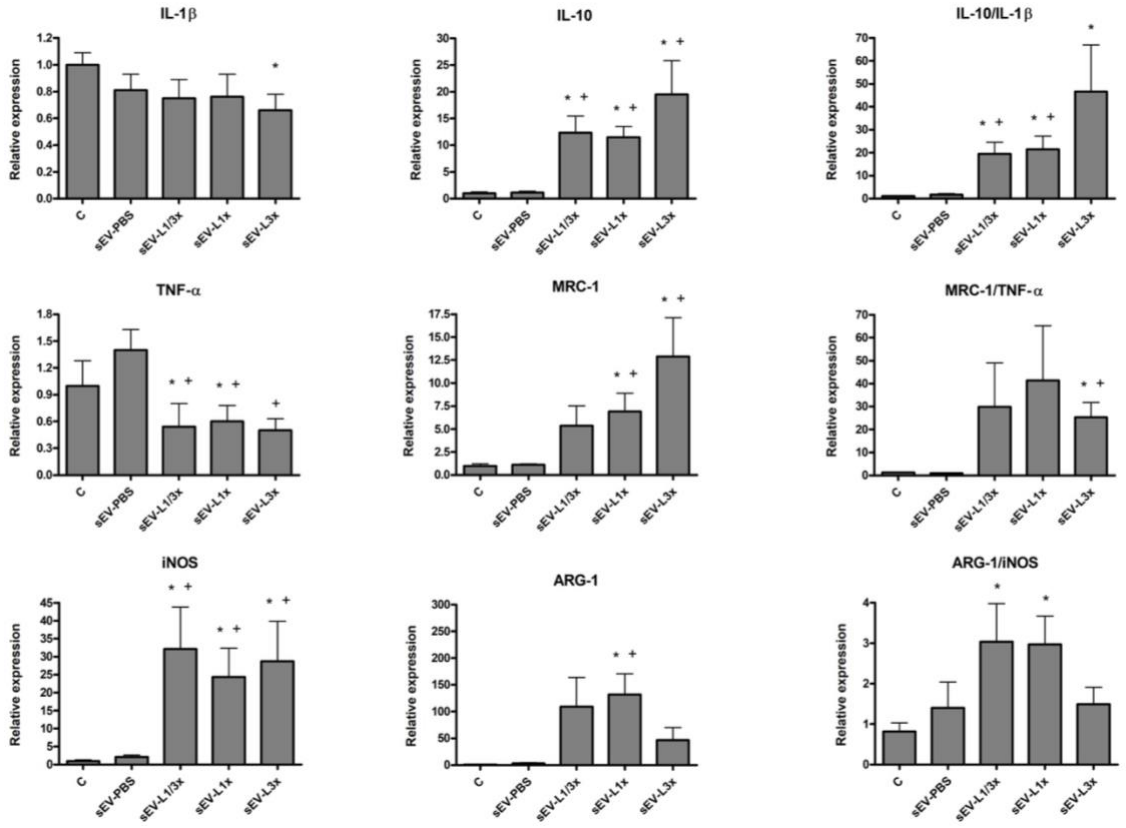

*Figure 10: Relative expression levels of IL-1β, IL-10, TNF-α, MRC-1, iNOS and ARG-1 in THP-1-derived macrophages treated with sEVs previously incubated with PBS (PBS) or three lactate treatments: L1/3x, L1x and L3x. Control cells (C) were not exposed to sEVs. In all cases, cells were incubated with the respective treatment for 5 hours. *p<0.05 vs Control; +p<0.05 vs sEV-PBS.*

4.3.3 Impact of lactate treatment duration on exosomes

Following the observed tendency towards M2 phenotype in the previous assay, we investigated whether the inflammatory response of macrophages was influenced by the duration of exosome incubation with lactate. To do so, macrophages were treated with sEVs that had been incubated with PBS (negative control) or lactate for different time periods (10 minutes, 1 hour, 5 hours or 24 hours). After treatment, we evaluated the expression levels of the same set of genes analyzed previously.

The results (Figure 11) revealed a similar pattern to the prior findings: M1-associated markers tended to decrease, while M2 markers exhibited a rising trend. This polarization profile was further confirmed by an increased M2/M1 ratio in macrophages treated with sEVs exposed to lactate compared to those receiving with PBS.

Despite considerable dispersion in the data, the changes in macrophage response were already evident after just 10 minutes of exosome incubation with lactate.

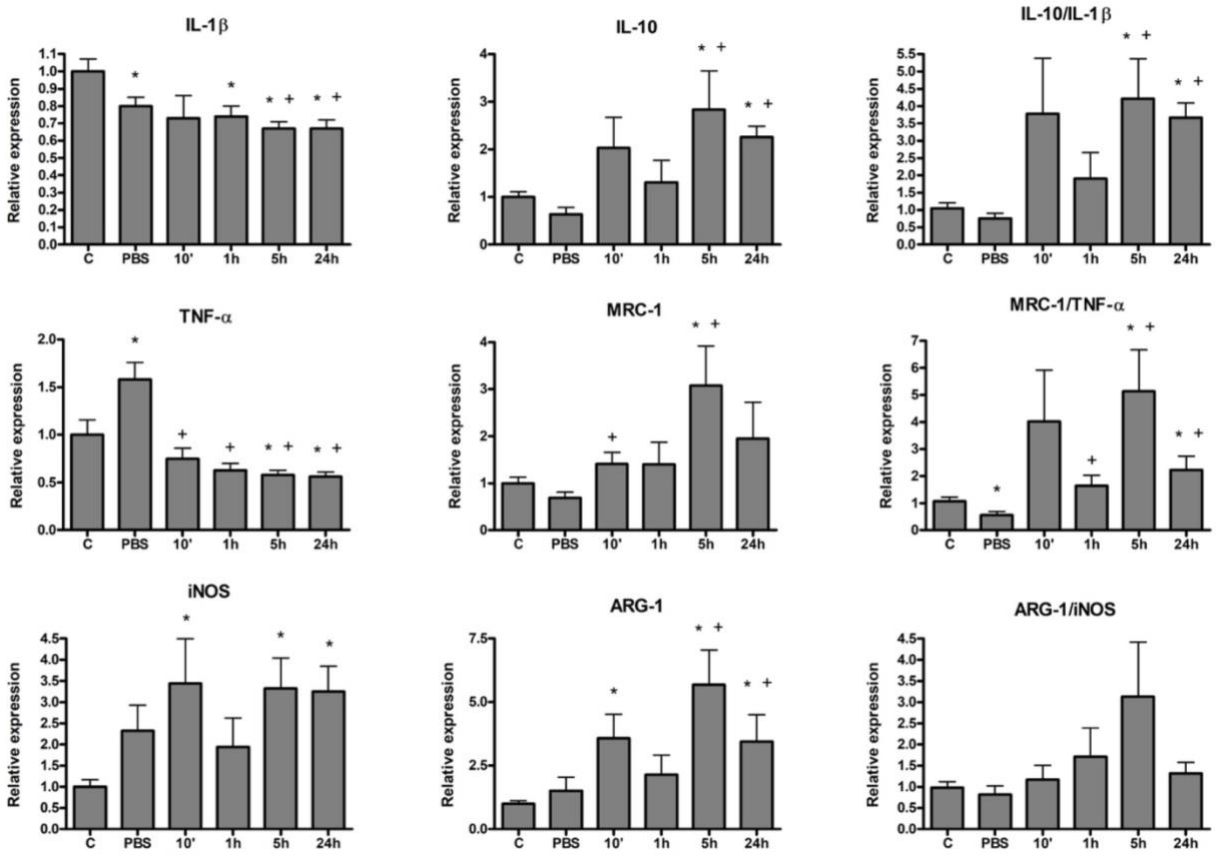

*Figure 11: Relative expression levels of IL-1β, IL-10, TNF-α, MRC-1, iNOS and ARG-1 in THP-1-derived macrophages treated with sEVs previously incubated with either PBS (PBS) for 0 minutes or lactate for 10 minutes (10'), 1 hour (1h), 5 hours (5h), or 24 hours (24h). Control cells (C) were not exposed to sEVs. In all cases, cells were incubated with the respective treatment for 5 hours. *p<0.05 vs Control; +p<0.05 vs sEV-PBS.*

4.3.4 Potential STAT3 signal transduction pathway

Considering the observed upregulation of classical M2 macrophage markers, and given that the JAK/STAT3 signaling pathway is one of the main transduction pathways involved in the shift of macrophages towards the M2 phenotype[31,32], we aimed to evaluate the activation of this pathway by determining the subcellular localization of STAT3 through immunofluorescence analysis.

Immunofluorescence images (Figure 12) show that STAT3 remains predominantly in a cytoplasmic distribution in both sEV-PBS and sEV-L_{1x} treated cells.

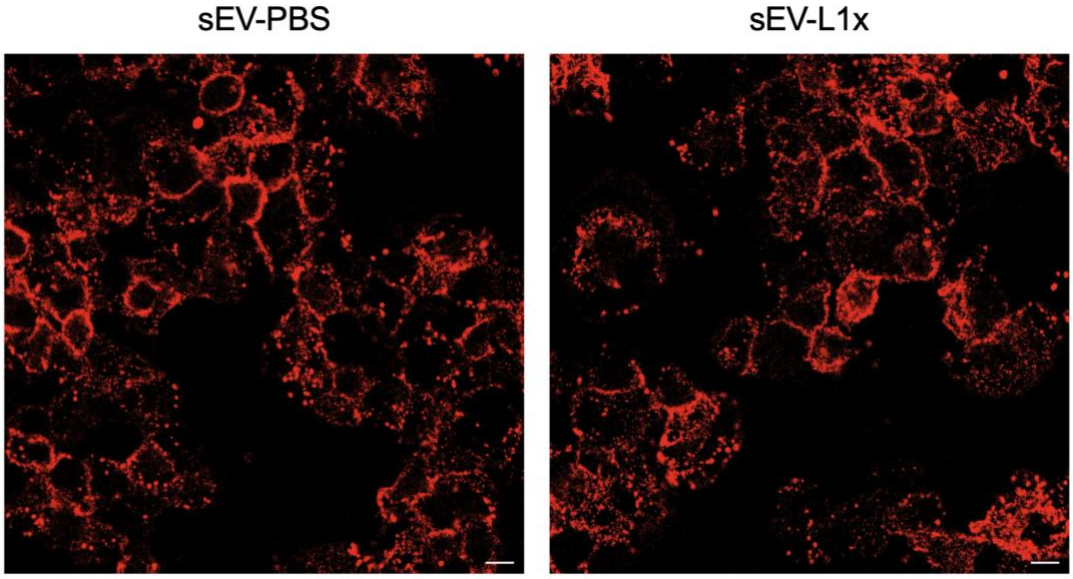

Figure 12: Fluorescence microscopy analysis of STAT3 localization in THP-1-derived macrophages. Cells were treated with 10µg/ml of sEV-PBS or sEV-L1x for one and a half hours. No nuclear translocation of STAT3 was observed in either condition. Scale bar: 10 µm.

4.3.5 Exosomes uptake by macrophages

Given the observed differences in gene expression in macrophages treated with sEV-L_{1x}, we sought to determine whether these changes could be related to differences in exosome uptake by macrophages.

To explore this, macrophages were incubated for 1 hour with sEV-L_{1x} or sEV-PBS. Fluorescence microscopy images (Figures 13 and 14) revealed no significant differences in exosome uptake between the two groups. The intracellular fluorescence signal was comparable, proposing that lactate exposure does not affect the ability of exosomes to be internalized by macrophages.

This was further confirmed by calculating the percentage of cells that had internalized exosomes in each condition: 56% (±6.6) of sEV-PBS-treated cells and 53% (±7.2) of cells treated with sEV-L_{1x}.

Images are first shown separately for each fluorescence channel, followed by a merged image combining nucleus and exosome signal.

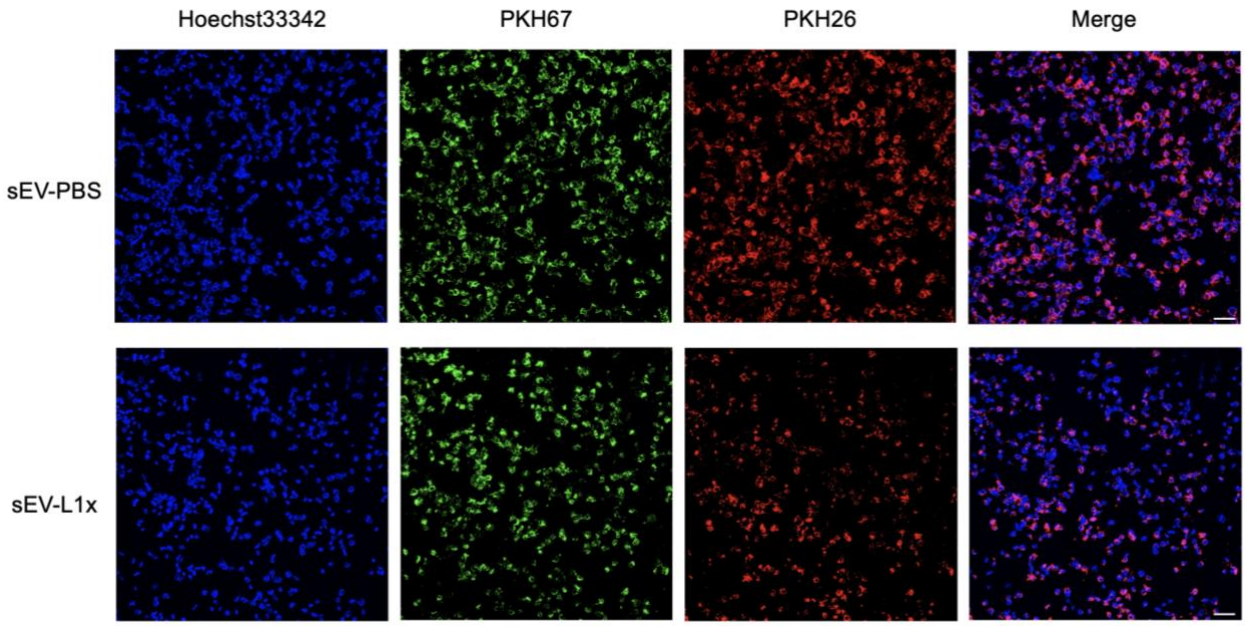

Figure 13: Fluorescence microscopy analysis of exosome uptake by THP-1-derived macrophages. Cells were labeled with PKH67 (green) and treated with for 1 hour with 10µg/ml of sEV-PBS or sEV-L1x, both labeled with PKH26 (red). Cell nuclei were stained in blue with Hoechst33342. Merged images show no appreciable differences in exosome internalization between conditions. Scale bar: 50 µm.

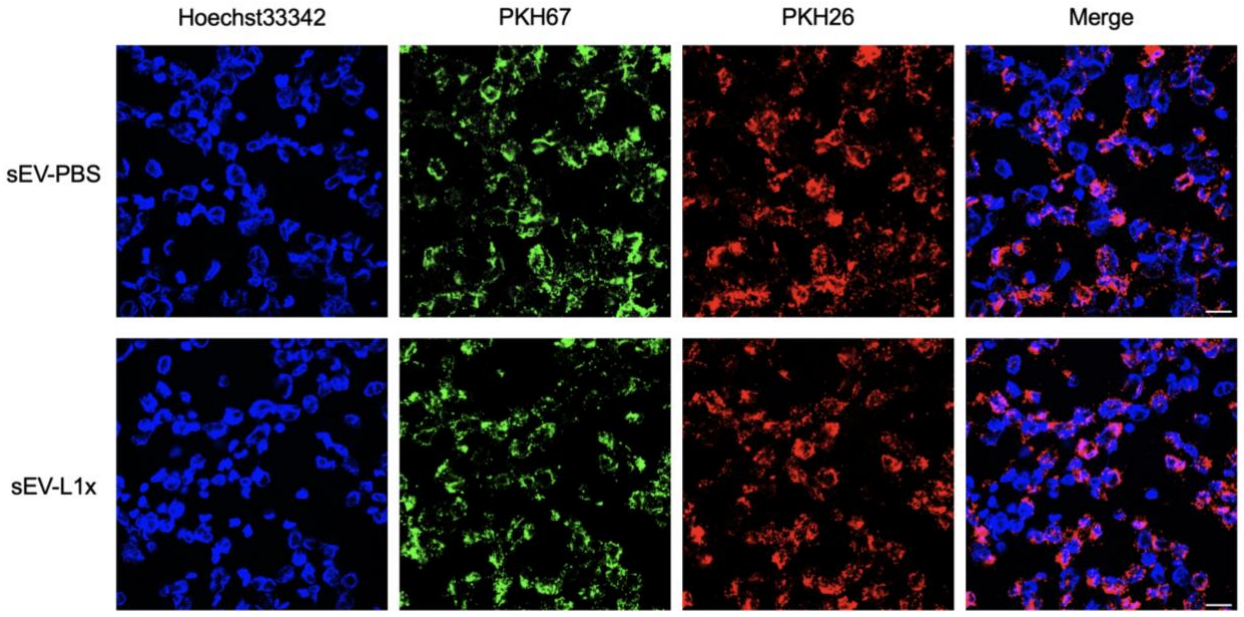

Figure 14: Fluorescence microscopy analysis of exosome uptake by THP-1-derived macrophages. Cells were labeled with PKH67 (green) and treated with for 1 hour with 10µg/ml of sEV-PBS or sEV-L1x, both labeled with PKH26 (red). Cell nuclei were stained in blue with Hoechst33342. Merged images show no appreciable differences in exosome internalization between conditions. Scale bar: 20µm.

5. Discussion and conclusions

Isolating sEVs, such as exosomes, is a challenging and time-consuming process, but also essential to carry out our experiments. One of the main challenges in exosome isolation is the potential co-precipitation with soluble proteins, which can compromise the purity of the final preparation[33]. To evaluate the effectiveness of our laboratory protocol in removing these contaminants, we analyzed the supernatant fractions collected during different steps of the isolation process. From this samples, we determined the concentration of soluble proteins and calculated the total number of proteins presents in the full sample volume at each step. This allowed us to estimate the percentage of protein contaminants removed throughout the protocol. The results demonstrated the progressive enrichment of sEVs relative to soluble protein content throughout the isolation procedure, highlighting the high effectiveness in purifying sEVs of the method.

Another critical limitation of the sEV isolating process is the low concentration of sEVs finally obtained[33]. After confirming that our isolation method effectively removed the vast majority of soluble proteins (>98%), we next focused on optimizing the protocol to increase the recovery of sEVs. Based on prior evidence from our laboratory that 5-hour ultracentrifugation improves the final concentration of sEVs, we adopted a combined protocol: an initial 16-hour (overnight) ultracentrifugation followed by a second 5-hour ultracentrifugation. This approach was compared with the original 2-hour + 2-hour method to test if extending the ultracentrifugation duration could improve the sEV recovery.

The results clearly demonstrated that the 16h + 5h protocol increased the final number of isolated sEVs, even though it started with a lower initial particle number. Notably, this enhanced method allowed for the recollection of nearly all particles present in the sample after the filtration step, indicating a high isolation efficiency. This improvement can be attributed to the use of large-volume ultracentrifugation tubes (27 ml), which require longer ultracentrifugation times to ensure complete sedimentation of sEVs. Extending the ultracentrifugation time allowed the recovery of a greater proportion of vesicles that would have remained incompletely sedimented after 2 hours. Additionally, the last ultracentrifugation step reduced the presence of larger particles (>200 nm), contributing to purer sEV population.

This suggests that extending the ultracentrifugation time not only increases the number of isolated sEVs but also enhances the quality and uniformity of the final preparation. From that point forward, the sEV isolation method in our laboratory was updated to the 16h + 5h protocol, which achieves an optimal balance between sEV yield and purity, while maintaining an efficient laboratory workflow.

Cellular experiments were initiated once the sEV isolation protocol had been optimized and the vesicles obtained had been confirmed to correspond to sEVs through standard characterization methods, including particle number, size distribution, and marker expression.

Our interest in studying the changes in macrophage gene expression after treating them with exosomes previously incubated with lactate was motivated by the anti-inflammatory properties of lactate observed in previous studies[28,29]. To this end, sEVs were exposed to PBS or to the same

concentration of lactate as that present in LR. Macrophages were then treated with these sEVs, and after 5 hours, we measured the expression levels of two classical M1 markers (*TNF-α* and *IL-1β*). Findings indicated an upregulation of both markers in response to sEV-PBS, which was mitigated by lactate-treated exosomes. Interestingly, sEVs alone appeared to induce a mild pro-inflammatory response, possibly due to the stress conditions under which they were collected. The 72-hour incubation in FBS-free medium could have induced cellular stress similar to a fasting state, thereby influencing the biological properties of exosomes.

Following the previous results, we wondered whether the observed reduction in M1-related genes in macrophages treated with sEV-L_{1x} was not merely due to lower macrophage activation, but rather indicative of a potential phenotypic shift. For this reason, we decided to investigate the expression levels of typical M1 and M2 macrophage markers. Additionally, we analyzed the ratios between M2 and M1 markers to determine whether one phenotype was predominant over the other, and the resulting ratios revealed a clear shift towards the M2 phenotype. We also evaluated whether the concentration of lactate used to treat exosomes could influence gene expression levels in macrophages.

While the increase of classical M2 markers in cells treated with sEV-L was not directly proportional to lactate concentrations, their levels were clearly increased compared to M1 markers. These findings pointed to the possibility that lactate could be promoting a phenotypic switch in macrophages from M1 to M2.

Although *iNOS* is a classical M1 marker and its expression appeared to increase, the overall M2/M1 ratio was still elevated in sEV-L-treated cells compared to both controls (C and sEV-PBS). This suggests that the upregulation of M2 markers was more pronounced than that of M1 markers. Additionally, it is important to consider that prior to treatment, macrophages were deprived of FBS, which can induce cellular stress and alter the molecular profile of exosomes[34].

After observing a potential shift of macrophages towards M2 phenotype, we sought to determine if the extent of this polarization was influenced by the duration of sEVs exposed to lactate. for this, exosomes were incubated with lactate at the concentration present in LR and time periods varied before treating macrophages with these sEVs. Results supported our previous findings, showing an overall increase in M2 markers relative to M1 markers. However, this tendency did not follow a proportional correlation with the incubation time of exosomes with lactate.

STAT3 is a transcription factor involved in multiple signaling pathways, including those associated with macrophages polarization towards M2 phenotype[31]. Upon activation, STAT3 becomes phosphorylated, triggering its dimerization and subsequent translocation to the nucleus, where it regulates the transcription of target genes[32]. Therefore, we performed an experiment to investigate whether the effect observed with lactated-treated exosomes was associated with STAT3 pathway activation. Nevertheless, our data show that STAT3 pathway was not activated due to it remained in the cytoplasm in both treatment conditions (sEV-PBS and sEV-L_{1x}). These findings suggest that STAT3 pathway does not underlie the phenotypic shift, indicating that a different signaling pathway may be mediating the observed changes in gene expression.

In Figure 13, it may seem that macrophages treated with control exosomes (sEV-PBS) exhibit increased uptake compared to those treated with sEV-L_{1x}. However, this apparent difference is attributable to a lower number of cells present in the sEV-L_{1x} field. In contrast, the higher-magnification image (Figure 14) allows for a more accurate comparison and reveals that the uptake of exosomes is similar between both conditions. The uptake quantification shows a very similar percentage between both treatments, indicating no differences between them. These findings suggests that apparently, the modifications induced by lactate have no impact on exosome internalization by macrophages. Therefore, the altered gene expression induced by sEV-L_{1x} is not due to differences in exosome uptake.

Altogether, these findings highlight a potential mechanism by which lactate present in LR has anti-inflammatory properties compared to NS in AP treatment. However, the precise mechanism through which lactate induces these effects remains unclear and requires further investigation.

Conclusions

Although the initial methodology for exosomes isolation proved to be excellent in terms of purity, we improved the total number of sEVs collected in the final sample.

Exposure of exosomes to lactate results in modifications of gene expression patterns in macrophages treated with these exosomes.

No correlation was observed between lactate concentration and the changes in the effect of exosomes on the gene expression profile of macrophages.

Incubating exosomes with lactate for 10 minutes is enough to observe changes in their effects on macrophage gene expression.

The switch to the M2 macrophage phenotype does not seem to be mediated by activation of STAT3 signaling transduction pathway.

Lactate-induced modifications on exosomes does not modify their uptake by macrophages.

6. Bibliography

1. Chen L, Deng H, Cui H, et al. Inflammatory responses and inflammation-associated diseases in organs. *Oncotarget*. 2017;9(6):7204-7218. doi:10.18632/oncotarget.23208

2. Ryu S, Lee EK. The Pivotal Role of Macrophages in the Pathogenesis of Pancreatic Diseases. *Int J Mol Sci*. 2024;25(11):5765. doi:10.3390/ijms25115765

3. Shapouri-Moghaddam A, Mohammadian S, Vazini H, et al. Macrophage plasticity, polarization, and function in health and disease. *Journal of Cellular Physiology*. 2018;233(9):6425-6440. doi:10.1002/jcp.26429

4. Wang N, Liang H, Zen K. Molecular Mechanisms That Influence the Macrophage M1–M2 Polarization Balance. *Front Immunol*. 2014;5:614. doi:10.3389/fimmu.2014.00614

5. Jeppesen DK, Zhang Q, Franklin JL, Coffey RJ. Extracellular Vesicles and Nanoparticles: Emerging Complexities. *Trends Cell Biol*. 2023;33(8):667-681. doi:10.1016/j.tcb.2023.01.002

6. Moghassemi S, Dadashzadeh A, Sousa MJ, et al. Extracellular vesicles in nanomedicine and regenerative medicine: A review over the last decade. *Bioact Mater*. 2024;36:126-156. doi:10.1016/j.bioactmat.2024.02.021

7. Isaac R, Reis FCG, Ying W, Olefsky JM. Exosomes as mediators of intercellular crosstalk in metabolism. *Cell Metab*. 2021;33(9):1744-1762. doi:10.1016/j.cmet.2021.08.006

8. Kalluri R, LeBleu VS. The biology, function, and biomedical applications of exosomes. *Science*. 2020;367(6478):eaau6977. doi:10.1126/science.aau6977

9. Krylova SV, Feng D. The Machinery of Exosomes: Biogenesis, Release, and Uptake. *Int J Mol Sci*. 2023;24(2):1337. doi:10.3390/ijms24021337

10. Gurung S, Perocheau D, Touramanidou L, Baruteau J. The exosome journey: from biogenesis to uptake and intracellular signalling. *Cell Commun Signal*. 2021;19:47. doi:10.1186/s12964-021-00730-1

11. Wei H, Chen Q, Lin L, et al. Regulation of exosome production and cargo sorting. *Int J Biol Sci*. 2021;17(1):163-177. doi:10.7150/ijbs.53671

12. Zhang Y, Liu Y, Liu H, Tang WH. Exosomes: biogenesis, biologic function and clinical potential. *Cell Biosci*. 2019;9:19. doi:10.1186/s13578-019-0282-2

13. De Toro J, Herschlik L, Waldner C, Mongini C. Emerging Roles of Exosomes in Normal and Pathological Conditions: New Insights for Diagnosis and Therapeutic Applications. *Front Immunol*. 2015;6:203. doi:10.3389/fimmu.2015.00203

14. Paskeh MDA, Entezari M, Mirzaei S, et al. Emerging role of exosomes in cancer progression and tumor microenvironment remodeling. *J Hematol Oncol*. 2022;15:83. doi:10.1186/s13045-022-01305-4

15. Exosomes in Inflammation and Inflammatory Disease - Chan - 2019 - PROTEOMICS -

Wiley Online Library. Accessed June 10, 2025. https://analyticalsciencejournals.onlinelibrary.wiley.com/doi/10.1002/pmic.201800149

16. Heidarzadeh M, Zarebkohan A, Rahbarghazi R, Sokullu E. Protein corona and exosomes: new challenges and prospects. *Cell Commun Signal*. 2023;21:64. doi:10.1186/s12964-023-01089-1

17. Tóth EÁ, Turiák L, Visnovitz T, et al. Formation of a protein corona on the surface of extracellular vesicles in blood plasma. *J Extracell Vesicles*. 2021;10(11):e12140. doi:10.1002/jev2.12140

18. Armengol-Badia O, Maggi J, Casal C, et al. The Microenvironment in an Experimental Model of Acute Pancreatitis Can Modify the Formation of the Protein Corona of sEVs, with Implications on Their Biological Function. *International Journal of Molecular Sciences*. 2024;25(23):12969. doi:10.3390/ijms252312969

19. Dietz L, Oberländer J, Mateos-Maroto A, et al. Uptake of extracellular vesicles into immune cells is enhanced by the protein corona. *J Extracell Vesicles*. 2023;12(12):e12399. doi:10.1002/jev2.12399

20. Fazeli A, Godakumara K. The evolving roles of extracellular vesicles in embryo-maternal communication. *Commun Biol*. 2024;7(1):754. doi:10.1038/s42003-024-06442-9

21. Weiss FU, Laemmerhirt F, Lerch MM. Etiology and Risk Factors of Acute and Chronic Pancreatitis. *Visc Med*. 2019;35(2):73-81. doi:10.1159/000499138

22. Wiley MB, Mehrotra K, Bauer J, Yazici C, Bialkowska AB, Jung B. Acute Pancreatitis. *Pancreas*. 2023;52(6):e335-e343. doi:10.1097/MPA.0000000000002259

23. Garg PK, Singh VP. Organ Failure due to Systemic Injury in Acute Pancreatitis. *Gastroenterology*. 2019;156(7):2008-2023. doi:10.1053/j.gastro.2018.12.041

24. Singh VK, Wu BU, Bollen TL, et al. Early Systemic Inflammatory Response Syndrome Is Associated With Severe Acute Pancreatitis. *Clinical Gastroenterology and Hepatology*. 2009;7(11):1247-1251. doi:10.1016/j.cgh.2009.08.012

25. Classification of acute pancreatitis—2012: revision of the Atlanta classification and definitions by international consensus | Gut. Accessed May 26, 2025. https://gut.bmj.com/content/62/1/102.long

26. Involvement of exosomes in lung inflammation associated with experimental acute pancreatitis - Bonjoch - 2016 - The Journal of Pathology - Wiley Online Library. Accessed June 10, 2025. https://pathsocjournals.onlinelibrary.wiley.com/doi/10.1002/path.4771

27. Gea-Sorlí S, Closa D. Role of macrophages in the progression of acute pancreatitis. *World J Gastrointest Pharmacol Ther*. 2010;1(5):107-111. doi:10.4292/wjgpt.v1.i5.107

28. Guilabert L, Cárdenas-Jaén K, Vaillo-Rocamora A, et al. Normal saline versus lactated Ringer's solution for acute pancreatitis resuscitation, an open-label multicenter randomized controlled trial: the WATERLAND trial study protocol. *Trials*. 2024;25(1):699.

doi:10.1186/s13063-024-08539-2

29. Fluid resuscitation with lactated Ringer's solution vs normal saline in acute pancreatitis: A triple-blind, randomized, controlled trial - Enrique de-Madaria, Iván Herrera-Marante, Verónica González-Camacho, Laia Bonjoch, Noé Quesada-Vázquez, Isabel Almenta-Saavedra, Cayetano Miralles-Maciá, Nelly G Acevedo-Piedra, Manuela Roger-Ibáñez, Claudia Sánchez-Marin, Rosa Osuna-Ligero, Ángel Gracia, Pere Llorens, Pedro Zapater, Vikesh K Singh, Rocío Moreu-Martín, Daniel Closa, 2018. Accessed May 23, 2025. https://journals.sagepub.com/doi/10.1177/2050640617707864

30. Singh M, Tiwari PK, Kashyap V, Kumar S. Proteomics of Extracellular Vesicles: Recent Updates, Challenges and Limitations. *Proteomes*. 2025;13(1):12. doi:10.3390/proteomes13010012

31. Li M, Wang M, Wen Y, Zhang H, Zhao G, Gao Q. Signaling pathways in macrophages: molecular mechanisms and therapeutic targets. *MedComm (2020)*. 2023;4(5):e349. doi:10.1002/mco2.349

32. Xia T, Zhang M, Lei W, et al. Advances in the role of STAT3 in macrophage polarization. *Front Immunol*. 2023;14:1160719. doi:10.3389/fimmu.2023.1160719

33. Jia Y, Yu L, Ma T, et al. Small extracellular vesicles isolation and separation: Current techniques, pending questions and clinical applications. *Theranostics*. 2022;12(15):6548-6575. doi:10.7150/thno.74305

34. Ludwig N, Whiteside TL, Reichert TE. Challenges in Exosome Isolation and Analysis in Health and Disease. *Int J Mol Sci*. 2019;20(19):4684. doi:10.3390/ijms20194684

7. Supplementary material

PRIMER	FORWARD SEQUENCE (5'>3')	REVERSE SEQUENCE (5'>3')
GAPDH	GATCATGAGCAATGCCTCCT	TGTGGTCATGAGTCGTTCCA
IL-1β	GGACAAGCTGAGGAAGATGC	TCGTTATCCCATGTGTCGAA
TNF-α	GCCCATGTTGTAGCAAACC	GGCACCACCAACTGGTTATC
IL-6	TACCCCCAGGAGAAGATTCC	TTTTCTGCCAGTGCCTCTTT
iNOS	CACCATCCTGGTGGAACTCT	TCCAGGATACCTTGGACCAG
IL-10	GCTCCCTGGTTTCTCTTCCT	GTTCTTTGGGGAGCCAACAG
MRC-1	TCTGGTAGGAAACGCTGGTC	GGATGGATGGCTCTGGTG
ARG-1	TCCACGTCTCTCAAGCCAAT	ACACTCCACTGACAACCACA

Table S1: Specific human primers.

STEP	TEMPERATURE AND TIME
DNA polymerase activation	95°C for 1 minute and 30 seconds
40 cycles of amplification:	95°C for 15 seconds
Denaturation	95°C for 15 seconds
Annealing	60°C for 30 seconds
Extension	72°C for 20 seconds
Melting curve	From 55°C to 95°C, every 0.5°C

Table S2: qPCR protocol.